# Photon soliton and fine structure due to nonlinear Compton scattering

Carlos Montes
*Laboratoire de Physique de la Matière Condensée, Parc Valrose, 06034 Nice Cedex, France*
*and Observatoire de Nice, B. P. 252, 06007 Nice Cedex, France*
(Received 10 March 1976; revised manuscript received 26 February 1979)

Induced Compton scattering of high-intensity radiation, $N(\nu,t) = c^2 I(\nu,t)/2h\nu^3 \gg 1$, by a plasma is governed by a nonlinear integro-differential kinetic equation of the Boltzmann type. For a Maxwellian electron distribution, the transition probability kernel takes the form $K(\nu,\nu') \propto (\nu - \nu')$ $\exp[-(\nu-\nu')^2/2(\Delta\overline{\nu}_D)^2]$, where $\nu$ and $\nu'$ are the photon frequencies before and after scattering and $\Delta\overline{\nu}_D = [(2kT_e/m_ec^2)(1-\cos\alpha)]^{1/2}\nu$ is the Doppler width associated with the scattering angle $\alpha$. Only limiting cases with local approximative forms of the kernel have been treated up to now: for a broad photon spectrum ($\delta\nu \gg \Delta\overline{\nu}_D$) the kinetic equation was approximated by the Kompaneets differential equation corresponding to $K(\nu,\nu') \propto \delta'(\nu-\nu')$; for a narrow photon spectrum ($\delta\nu \ll \Delta\overline{\nu}_D$), the kernel was approximated by $K(\nu,\nu') \propto (\nu-\nu')$. Qualitative red-shift evolutions of particular initial spectrum profiles were found. Here, the general integro-differential kinetic equation which governs the nonlinear and nonlocal interaction between photons and electrons is studied by a numerical treatment and asymptotic analytical approaches are exhibited. Starting from several initial conditions—narrow or broad spectrum profiles, in the presence or in the absence of a noise spectrum—general spectral evolutions for one-dimensional conservative photon systems are obtained. In the presence of a constant noise spectrum $N_0$ a universal asymptotic solution of the soliton type is obtained: Whatever the initial conditions, a narrow photon spectrum $N(\nu,t)$ evolves towards a photon soliton moving downwards in the frequency axis with the form $\ln[N(\nu,t)/N_0] = [\ln(N_m/N_0)]\exp\{-[(\nu_S - \sigma t - \nu)^2/2(\Delta\overline{\nu}_D)^2\}$, where $N_m$ is the maximum amplitude and $\sigma = \text{const}(N_m - N_0)[\ln(N_m/N_0)]^{-3/2}$ is the speed. A broad spectrum, however, is decomposed into a set of such solitons which are ordered by amplitude (proportional to their speeds) in their downward motion. In the absence of a constant noise spectrum, an initial narrow Gaussian profile moves downwards (on the $\nu$ axis) with decreasing speed, growing in amplitude and narrowing in width.

## I. INTRODUCTION

The nonlinear induced and incoherent Compton scattering of high-intensity radiation by the plasma either by free thermal electrons or with allowance for screening of the ions, has been recently considered in the literature,[1-24] especially in connection with the study of powerful compact astronomical radio sources[6-11] or with laser-fusion laboratory experiments.[12-20] In a previous work,[24] I have suggested this nonlinear mechanism in order to interpret the strong variability of intensity observed in interstellar maser spectra in the light of a similar problem previously treated, namely, the relaxation kinetics for an unstable spectrum of plasmons interacting via nonlinear Landau damping with plasma ions.[25]

In a rarefied plasma, the interaction between a photon gas and an electron gas, giving rise to single-photon emission and absorption and to nonlinear induced Compton scattering is described by two integrodifferential kinetic equations of the Boltzmann type,[2,5] one for the photon occupation number $N(\nu,\hat{\Omega},t)$ and the other for the electron distribution function $f(\vec{p},t)$. Assuming spatial homogeneity, absence of collective plasma effects, and classical electrons (i.e., no quantum-statistical correlations between them), we write these

$$\frac{\partial N(\nu,\hat{\Omega},t)}{\partial t} = \int_0^\infty \nu'^2\, d\nu' \int d\hat{\Omega}' \int d\vec{p}\,\sigma(\vec{p},\vec{\nu}\to\vec{p}',\vec{\nu}')\{N(\vec{\nu}',t)[1+N(\vec{\nu},t)]f(\vec{p}',t) - N(\vec{\nu},t)[1+N(\vec{\nu}',t)]f(\vec{p},t)\}, \quad (1)$$

$$\frac{\partial f(\vec{p},t)}{\partial t} = \int_0^\infty \nu^2\, d\nu \int d\hat{\Omega} \int d\vec{p}'\,\sigma(\vec{p},\vec{\nu}\to\vec{p}',\vec{\nu}')\{N(\vec{\nu}',t)[1+N(\vec{\nu},t)]f(\vec{p}',t) - N(\vec{\nu},t)[1+N(\vec{\nu}',t)]f(\vec{p},t)\}, \quad (2)$$

where $\hat{\Omega}$ is the unit vector in the direction of propagation of photon $\nu$, $\vec{\nu}$ stands for $\nu\hat{\Omega}$, $\vec{p}$ is the electron momentum, and $\sigma(\vec{p},\vec{\nu}\to\vec{\nu}',\vec{p}')$ is the Klein-Nishina cross section in the frame where the electron is at rest, including the momentum and energy conservation relations. Since photons obey Bose-Einstein statistics, the induced Compton scattering term is characterized by a transition probability proportional to $N(\vec{\nu},t)+1$ and may dominate over the linear Compton scattering if $N(\vec{\nu},t)$

 © 1979 The American Physical Society

$\gg 1$, more precisely if

$$\Omega_0 \frac{\delta\nu}{\nu} \frac{N(\vec{\nu}, t)h\nu}{kT_e} \gg 1,$$

where $\Omega_0$ is the solid angle through which radiation of spectral width $\delta\nu$ travels.

Although the kinetic equations and transition probability for the nonlinear Compton interaction are already well established,[1-5,14] a detailed investigation of the general nonlinear integrodifferential equation governing the kinetics of $N(\vec{\nu}, t)$ has, to my knowledge, not yet been accomplished. Only limiting cases with local approximative forms of the transition-probability kernel have been treated until now. The simplified approaches, however, have described some outstanding effects of the nonlinear interaction and in a certain manner the qualitative features of the fine kinetic description. Among these effects may be mentioned the distortion of the initial electromagnetic spectrum of high-brightness temperature, which shifts towards lower frequencies and therefore heats the electrons,[5,6,14,21] the appearance of an induced force due to the pressure of light,[9] the formation of narrow spectral lines in an initially broad spectrum,[8,15] and the evolution of spectrally narrow lines depending on its spectral profiles.[14] The Bose condensation of the photon gas due to the induced Compton transfer of the photon spectrum towards lower frequencies has also been considered recently.[8,10,22,23]

We are only interested here in the photon kinetics, and I shall assume throughout that the electrons are Maxwellian at temperature $T_e$. Even though the starting kinetic equation will be rederived in Sec. II from Eq. (1) we may write it here for comparison with previous approaches. The kinetic equation for the photon occupation number $N(\vec{\nu}, t)$ reads

$$\frac{\partial N(\vec{\nu}, t)}{\partial t} = \mathfrak{L}[N(\vec{\nu}, t)] - \frac{3}{16\pi} n_e c\sigma_T N(\vec{\nu}, t) \int \nu'^2 d\nu' \int d\hat{\Omega} \times (1+\cos^2\alpha) K(\nu, \nu', \alpha) N(\vec{\nu}', t), \quad (3)$$

$\mathfrak{L}[N(\vec{\nu}, t)]$ being the linear contribution to the Compton scattering and $K(\nu, \nu', \alpha)$ the transition-probability kernel having the antisymmetrical form[14]

$$K(\nu, \nu', \alpha) = \frac{2h(\nu-\nu')}{\sqrt{2\pi}\, m_e c^2 (\Delta\nu_D)^3 (1-\cos\alpha)^{1/2}} \times \exp\left(-\frac{(\nu-\nu')^2}{2(\Delta\nu_D)^2(1-\cos\alpha)}\right) \simeq \frac{2h(1-\cos\alpha)^{1/2}}{\sqrt{2\pi}\, m_e c^2 \Delta\nu_D} \times \frac{\partial}{\partial\nu} \exp\left(-\frac{(\nu-\nu')^2}{2(\Delta\nu_D)^2(1-\cos\alpha)}\right), \quad (4)$$

where $\Delta\nu_D = (2kT_e/m_e c^2)^{1/2}(\nu\nu')^{1/2}$ is the Doppler width, $\alpha$ the scattering angle, $n_e$ and $m_e$ the electron density and mass, and $\sigma_T = \frac{8}{3}\pi(e^2/m_e c^2)^2$ the Thomson scattering cross section.

Particularly important is Kompaneets's[1] "hydrodynamic" approximation in the limit of a broad isotropic spectrum of width $\delta\nu \gg \Delta\nu_D(1-\cos\alpha)^{1/2}$. The derivative of the Gaussian function in (4) is approximated by $\delta'(\nu-\nu')$ and the integral kinetic equation (3) becomes the Compton Fokker-Planck differential equation

$$\frac{\partial N(\nu, t)}{\partial t} = \frac{n_e h\sigma_T}{m_e c} \frac{1}{\nu^2} \frac{\partial}{\partial\nu} \nu^4 \left( N(\nu, t)[N(\nu, t)+1] + \frac{kT_e}{h} \frac{\partial N(\nu, t)}{\partial\nu} \right). \quad (5)$$

We have elsewhere[26] generalized this equation to include, together with the Compton scattering on the electrons, the Raman scattering on the plasmons.[27] The nonlinear evolution, however, is still governed by the induced Compton term $N(\nu, t)\partial[\nu^2 N(\nu, t)]/\partial\nu$. This term tends to distort the spectrum by steepening its red side and shifting its maximum towards lower frequencies with a speed proportional to $N(\nu, t)$. The presence of the linear diffusion term in Eq. (5) prevents the solution from being multivalued. Reinisch[21] has studied in detail the triangular evolution which follows and which is described by a Burger's-type equation. For the strong nonlinear case without diffusion, Peyraud[5(c)] has made a previous attempt to prevent multivalued evolution by adding heuristically a dispersive term of the Korteweg-de Vries (KdV) type $\propto \partial^3 N(\nu, t)/\partial\nu^3$ to the nonlinear Kompaneets equation. He thus explains qualitatively a high-intensity laser experiment[13] which shows a breaking of the initial profile into secondary ones or "solitons" following the KdV terminology. In the light of the general evolution of the spectrum satisfying the exact kinetic equation (3) with the complete kernel (4) we shall see that this idea was meaningful.

For a narrow photon spectrum of width $\delta\nu \ll \Delta\nu_D(1-\cos\alpha)^{1/2}$ the differential approximation is no longer valid and the integral kinetic equation must be considered. Zel'dovich *et al.*[14] have studied the propagation of several narrow spectrum profiles within the "local approximation" for the kernel, namely, $K(\nu, \nu') \propto (\nu-\nu')$. Assuming that $|\nu-\nu'| \sim \delta\nu(1-\cos\alpha)^{1/2} \ll \Delta\nu_D$, we can approximate the exponential function in (4) by unity. As we shall see, this approximation can only describe the onset oi evolution and that only in the absence of any noise spectrum (cf. Sec. V). For pure nonlinear evolution, $\mathfrak{L}[N(\nu, t)] = 0$, these authors have shown that a narrow Gaussian profile moves downwards on the frequency axis without changing its

shape, that a Lorentz profile spreads, becomes asymmetric, and gradually disappears, and that a rectangular line profile becomes narrower and shifts towards the low-frequency edge. No universal behavior independent of initial shape was given.

In this paper I also study pure nonlinear Compton kinetics $\{N(\nu,t)\gg 1,\ \mathfrak{L}[N(\nu,t)]=0\}$, but I start from the general kinetic equation (3) with the complete transition-probability kernel (4), which governs the nonlinear and nonlocal interaction between photons and electrons and which must be considered as the master equation for induced or nonlinear Compton scattering. Starting from several initial conditions —narrow or broad spectrum profiles, in the presence or in the absence of a noise spectrum—I obtain general spectral evolutions for one-dimensional conservative photon systems. A high-amplitude oscillating kinetics in the presence of a linear source term was obtained previously.[24,28] So, in the presence of a white- (even extremely low-) noise spectrum $N_0$, the numerical integration of the kinetic equation (3) + (4) in the one-dimensional case [cf. Eq. (27)] leads to the following general behavior in the $(t,\nu)$ plane[28]:

(i) A narrow spectrum ($\delta\nu<\Delta\bar{\nu}_D$) transforms with time into one *photon soliton* of universal form which moves downwards on the frequency axis at constant speed $\sigma=d\nu/dt$ and constant amplitude. For a high rate, $N_m/N_0\gg 1$, of the maximum amplitude $N_m$ to the noise amplitude $N_0$, the photon soliton takes at each moment the form fitted by the transition-probability kernel (4), namely,

$$\ln\frac{N(\nu,t)}{N_0}=\ln\frac{N_m}{N_0}\exp\left[\left(\frac{\nu_s-\sigma t-\nu}{\sqrt{2}\,\Delta\bar{\nu}_D}\right)^2\right], \tag{6}$$

where $\Delta\bar{\nu}_D=\Delta\nu_D\langle(1-\cos\alpha)^{1/2}\rangle_\Omega$ is the Doppler width associated with the mean scattering direction $\alpha$ and $\nu_s$ is the frequency origin at which the soliton moves with amplitude $N_m$ and speed $\sigma\propto(N_m-N_0)[\ln(N_m/N_0)]^{-3/2}$. When the initial spectrum centered at $\nu=\nu_0$ is very narrow ($\delta\nu\ll\Delta\bar{\nu}_D$) it transforms first with time into a red Doppler satellite on the low-frequency side at frequency $\nu_s=\nu_0-\Delta\bar{\nu}_D$ which then behaves as a soliton of form (6).

(ii) A large spectrum ($\delta\nu>\Delta\bar{\nu}_D$) breaks with time into a set of such solitons. In their motion downwards on the $\nu$ axis, they are ordered by their amplitudes, or, equivalently, by their speeds, therefore increasing the distances between them. This shows that photon solitons are the basic elements composing any high electromagnetic spectrum in interaction with plasma electrons via nonlinear Compton scattering. Thus the nonlinear evolution reveals, in fact, the fine structure of the spectrum.

Note that the complete kernel's form (4) is essential for the buildup of the universal asymptotic form (6), because it ensures nonlinear and nonlocal coupling between the initial spectrum and the noise spectrum. Therefore soliton (6) cannot be obtained in the absence of a noise spectrum and within the local $\nu-\nu'$ approximation for $K(\nu,\nu')$.[14,15]

Moreover, even in the absence of a constant noise spectrum Eq. (3) with the complete kernel (4) leads to evolutions of initial spectra which differ from those obtained within the local approximation. For example, in the case of an initial narrow Gaussian profile ($\delta\nu\ll\Delta\bar{\nu}_D$), I find, unlike Zel'dovich *et al.*,[14] that it cannot remain invariant during its downward motion on the frequency axis. The numerical evolution shows that its speed decreases, its amplitude grows, and its width decreases. It seems like a solitary spectrum moving on a decreasing-amplitude "noise", which is nothing but its own low-frequency wing. The logarithmic dependence on the noise $N_0$ which soliton (6) exhibits becomes here a logarithmic dependence on the wing amplitude. An analytical asymptotic approach may thus be used to explain the whole spectral evolution, in particular the appearance of a second bump in the high-frequency side behind the main solitary spectrum.

After the present paper was first submitted for publication, I was informed by Zakharov, *et al.* of a recent paper,[29] now older, with the same optics as mine, devoted to the formally identical Langmuir turbulence problem. It should, however, be noted that on the one hand neither the analytic asymptotic form (6) for the soliton nor the correct expression for the soliton velocity $\sigma$ are given there. On the other hand, they propose two other dynamical models which may qualitatively describe the kinetics of the integral equation in the one-dimensonal case. One is the "peak kinetics" approximation obtained by replacing the kernel (4)—which has the form of the derivative of a Gaussian function—by $\delta(\nu-\nu'+\Delta\bar{\nu}_D)-\delta(\nu-\nu'-\Delta\bar{\nu}_D)$. Taking the initial spectrum as a linear sequence of peaks, $N(\nu)=\sum_{i=0}^{n}N_i\delta(\nu_0\pm n\Delta\bar{\nu}_D)$, they are led to the discrete feeder-eater Volterra equation

$$\frac{dN_i}{d\tau}=N_i(N_{i+1}-N_{i-1}), \tag{7}$$

which Manakov[30] has shown to be a perfectly integrable equation the solutions of which are solitons traveling along a chain of peaks. The second approximation proposed for a broad initial spectrum ($\delta\nu\gg\Delta\nu_D$) consists of replacing the kernel by the expansion $\delta'(\nu-\nu')+\frac{1}{2}(\Delta\bar{\nu}_D)\delta'''(\nu-\nu')$, which leads in fact to a KdV-like equation but with a nonlinear dispersive term, namely,

$$\frac{\partial N(\nu,\tau)}{\partial \tau} = N(\nu,\tau)\left(\frac{\partial}{\partial \nu} + \frac{(\Delta \bar{\nu}_D)^2}{2}\frac{\partial^3}{\partial \nu^3}\right) N(\nu,t), \quad (8)$$

with the reduced time $\tau$ containing the scattering cross section. Equation (8) was derived previously by Reinisch[31] and also presents soliton solutions in the presence of a noise spectrum. However, the soliton width is of the order of the expansion parameter $\Delta \bar{\nu}_D$, and no quantitative justification is available to keep the Gaussian expansion of the kernel (4) up to the second order in $\Delta \bar{\nu}_D$. Indeed, either the soliton velocity obtained from Eqs. (7) or (8) which is $\propto N_m/\ln N_m$ or the soliton shape and width differ from that I have obtained for the integral master Eq. (3) + (4) in the one-dimensional case, which is given by (6). Only qualitative kinetic evolutions in the form of solitons or multisolitons are common; these improve Peyraud's primitive idea of correcting the Kompaneet's differential equation (5) by the addition of a KdV dispersive term.

The integral master equation (3) + (4), however, seems to be a system which is not completely integrable; We have found only two exact integrals of motion.[32] In this sense the name soliton must be understood in the broad sense of an almost stable high-amplitude structure which moves with a velocity proportional to its amplitude, or following Makhankov,[33] we may generalize the definition of a soliton as a solitary wave having some "safety factor" which ensures a weak change in interaction or collision with others. In a recent paper[32] we have studied collisions between these photon solitons in order to test their structural stability. Paired collisions between photon solitons take place at a finite range in the same way as particles having a potential. The existence of two invariants of motion forces the two outgoing solitons to be equivalent to the incoming ones after exchanging their identities. Multiple soliton collisions violate the conservation of the number of solitons, e.g., ternary collisions show the rise of a fourth soliton structure.

## II. NONLINEAR INTEGRODIFFERENTIAL KINETIC EQUATION

We shall consider the evolution with time of an initial ensemble of photons interacting with an electron gas via the Compton collisions. We are only interested in the photon kinetics, and shall therefore assume that the electron gas is Maxwellian at temperature $T_e$. Thus the photon occupation number $N(\nu, \hat{\Omega}, t)$ in the direction of propagation $\hat{\Omega}$, defined by

$$N(\nu,\hat{\Omega},t) = c^2 I(\nu,\hat{\Omega},t)/2h\nu^3, \quad (9)$$

is governed by the nonlinear kinetic equation (1). $I(\nu,\hat{\Omega},t)$ is the spectral intensity of the radiation in a given solid angle $d\Omega = d\varphi \sin\theta\, d\theta$ and is related to the spectral energy density by

$$\epsilon(\nu,t) = \frac{1}{c}\int I(\nu,\hat{\Omega},t)\, d\hat{\Omega}.$$

Moreover, we shall consider the nonrelativistic case defined by inequalities

$$h\nu \ll kT_e \ll m_e c^2, \quad (10)$$

and we concern ourselves with the evolution of a high photon occupation number

$$N(\nu,\hat{\Omega},t) \gg 1, \quad (11)$$

which allows us to neglect the linear terms in the right-hand side of Eq. (1) and so to retain only the nonlinear induced Compton interaction. To obtain the starting kinetic equation (4) from the general equation (1) we introduce in Eq. (1) the momentum and energy conservation equations for the Compton collision to the lowest order with respect to the small parameters $h\nu/m_e c^2$ and $h\nu/kT_e$, namely,

$$(\nu-\nu')/(\nu\nu')^{1/2} = (\vec{p}/m_e c)\cdot(\hat{\Omega}-\hat{\Omega}'), \quad (12)$$

$$p^2/2m_e + h\nu = p'^2/2m_e + h\nu', \quad (13)$$

where the incident $\hat{\Omega}(\theta,\varphi)$ and scattered $\hat{\Omega}(\theta',\varphi')$ photon directions are related by

$$\cos\alpha = \cos\theta\cos\theta' + \sin\theta\sin\theta'\cos(\varphi-\varphi'). \quad (14)$$

One obtains[14,24] the following nonlinear kinetic equation

$$\frac{\partial N(\vec{\nu},t)}{\partial t} = -n_e c N(\vec{\nu},t)\int \nu'^2\, d\nu' \int d\hat{\Omega}\,\frac{d\sigma}{d\Omega} \times K(\nu,\nu',\alpha) N(\vec{\nu},t), \quad (15)$$

where $d\sigma/d\Omega$ is the differential cross section for scattering given by

$$\frac{d\sigma}{d\Omega} = \frac{3}{16\pi}\sigma_T(1+\cos^2\alpha), \quad (16)$$

and where the transition-probability kernel $K(\nu,\nu',\alpha)$ has the form (4), showing the antisymmetry with respect to replacement of $\vec{\nu}$ by $\vec{\nu}'$. Equation (15) therefore ensures the conservation in time of the total number of photons $\int d\Omega \int d\nu\, \nu^2 N(\nu,t)$ and has the explicit form (3) with the kernel (4).

Master equation (3) + (4) governs the kinetics in the $(t,\nu,\alpha)$ space, and one must perform a numerical computation to obtain complete information for the evolution in the general anisotropic

case, even if some approximative evolutions for a broad anisotropic spectrum have been already considered,[11,16] yielding a narrowing or spreading of the radiation beam. Let us limit ourselves here to a study of the more simple evolution in the $(t,\nu)$ plane along, which is the problem for the isotropic interaction between photons and electrons and may be a reasonable approximation for two anisotropic cases described in terms of a one-dimensional interaction geometry. Indeed, the absence[14] in the kernal $K(\nu,\nu',\alpha)$ of a singularity as $\nu \to \nu'$ permits replacement of the scattering angle $\alpha$—in the exponent of the kernel's expression (4)—by its more contributive value $\alpha_0$ to the integral of Eq. (3). Two limit cases are interesting: $\alpha_0 \ll 1$ and $\alpha_0 = \pi$. The first case corresponds to radiation collimated into a solid angle $\Omega_0 = \int_0^{2\pi} d\varphi \int_0^{\theta_0} \sin\theta\, d\theta$ of small aperture $2\theta_0$, so that $\alpha_0 \simeq \theta_0 \ll 1$. The second case corresponds to a total reflection of the incident photons and is only justified when the photon occupation number $N_{\rightarrow}(\vec{\nu},t)$ in the incident direction is as high as $N_{\leftarrow}(\vec{\nu},t)$ in the reflected direction. Then deflection through an angle $\alpha = \pi$ has maximum probability in Eq. (3), and therefore the nonlinear Compton interaction is accompanied by the backscattering, or induced Compton reflection of the radiation beam. This is the case when the radiation is isotropic, and may be also the case for two identical counterstreaming photon beams.[19,24] Then the photons will be trapped by the nonlinear Compton collisions and the medium becomes "nonlinearly" thick. In summary, the width of the Gaussian function in the kernel's expression (4), which associates the Doppler width $\Delta\nu_D$ to the more contributive scattering angle $\alpha_0$, defined by

$$\Delta\overline{\nu_D} = \Delta\nu_D (1-\cos\alpha_0)^{1/2}, \tag{17}$$

will be approximated by

$$\Delta\overline{\nu_D} = (\theta_0/\sqrt{2})\Delta\nu_D \quad (\alpha_0 = \theta_0 \ll 1) \tag{18}$$

for a small aperture radiation beam and by

$$\Delta\overline{\nu_D} = \sqrt{2}\,\Delta\nu_D \quad (\alpha_0 = \pi) \tag{19}$$

for isotropic or counterstreaming radiation.

Moreover, inasmuch as $|\nu-\nu'| \ll (\nu\nu')^{1/2} \ll \nu_0$, $\nu_0$ being the central frequency of the initial spectrum, we may approximate the Doppler width $\Delta\nu_D$ itself by the constant value

$$\Delta\nu_D = (2kT_e/m_ec^2)^{1/2}(\nu\nu')^{1/2} \simeq (2kT_e/m_ec^2)^{1/2}\nu_0. \tag{20}$$

Therefore the nonlinear integrodifferential kinetic equation which governs the inelastic induced Compton evolution with time in the homogeneous situation takes the form

$$\frac{\partial N(\nu,t)}{\partial t} = W\frac{N(\nu,t)}{\sqrt{2\pi}\,\Delta\nu_D}\int_0^{\infty} d\nu'\,\nu'^2 N(\nu',t) \times\left[\frac{\partial}{\partial\nu}\exp\left(-\frac{(\nu-\nu')^2}{2(\Delta\overline{\nu_D})^2}\right)\right], \tag{21}$$

where the dimensionless transition-probability coefficient is given by

$$W = \frac{n_e\sigma_T ch}{m_ec^2}\,a_{\theta_0}, \tag{22}$$

so that the angular contribution $a_{\theta_0}$ has been reduced to the evaluation of the factor

$$a_{\theta_0} = \frac{3}{8\pi}\left(\frac{\Delta\overline{\nu_D}}{\Delta\nu_D}\right)^3\int_0^{2\pi} d\varphi' \times\int_{\theta_1}^{\theta_2} d\theta' \sin\theta' \frac{1+\cos^2\alpha}{(1-\cos\alpha)^{1/2}}. \tag{23}$$

In the whole isotropic case, we have $\theta_1 = 0$, $\theta_2 = \pi$, $\cos\alpha = \cos\theta'$, and $\Delta\overline{\nu_D} = \sqrt{2}\,\Delta\nu_D$, yielding

$$a_{\theta_0}^{\text{isotr}} = \tfrac{44}{5}. \tag{24}$$

When the aperture angle of the radiation is small ($\theta_0 \ll 1$) we can obtain an order-of-magnitude estimate for the central region by putting $\theta = 0$ and therefore $\cos\alpha = \cos\theta'$, yielding for a small-aperture beam ($\theta_1 = 0$, $\theta_2 = \theta_0 \ll 1$), from (18)

$$a_{\theta_0}^{\text{beam}} = \tfrac{3}{4}\theta_0^4, \tag{25}$$

and for two identical counterstreaming beams ($\theta_1 = \pi - \theta_0$, $\theta_2 = \pi$) we have, from (19),

$$a_{\theta_0}^{\text{cs beams}} = 3\sqrt{2}\,\theta_0^2. \tag{26}$$

Equation (21) governs the nonlinear Compton kinetics for the one-dimensional (in frequency space) model. It can be transformed into the universal form

$$\frac{\partial N(x,\tau)}{\partial\tau} = \frac{N(x,\tau)}{\sqrt{\pi}}\int_{-\infty}^{+\infty} dx'\left(\frac{\partial}{\partial x}\exp[-(x-x')^2]\right)N(x',\tau) \tag{27}$$

by defining

$$N(x,\tau) = (\nu/\nu_0)^2 N(\nu,t), \tag{28}$$

$$\tau = t\,W\nu_0^2/\sqrt{2}\,\Delta\overline{\nu}_D, \tag{29}$$

$$x = \nu/\sqrt{2}\,\Delta\overline{\nu}_D, \tag{30}$$

where the reduced time $\tau$ is proportional to the transition-probability strength, the reduced frequency $x$ is proportional to $c/v_{th}$, $\nu_0$, measures the starting frequency, and the lower limit of the integral has been replaced by $-\infty$. This last simpli-

fication is only available for describing the kinetics when $x \gg 1$, which avoids the problem of photon condensation near $x = 0$.[8,10,22,23] Equation (27) has two exact invariants of motion,[32] namely,

$$I_1 = \int_{-\infty}^{+\infty} N(x,\tau)\, dx \equiv N, \tag{31}$$

$$I_2 = \int_{-\infty}^{+\infty} \ln N(x,\tau)\, dx, \tag{32}$$

but it does not seem to be an exactly integrable equation.[32] Invariant $I_1$ stands for the conservation of the total number of photons $N$. However, there is no conservation of the photon energy $\mathcal{E} \propto \int dx\, x N(x,\tau)$. The main action of the antisymmetric kernel of Eq. (27) is the transfer of photons towards lower frequencies (i.e., lower $x$). The loss of photon energy must be compensated by an increase in electron temperature in order to thermalize the high-brightness temperature of the photon spectrum. As noted before, we do not consider here this self-consistent problem, but only the nonstationary photon problem, assuming a constant temperature for the electron thermostat.

The nonlinear form of Eq. (27) shows at a glance the differing qualitative kinetics, depending upon whether the photon spectrum $N(x,\tau)$ takes or not a finite value overall on the $x$ axis; i.e., they depend on the noise spectrum. The nonlocal transfer towards lower frequencies would stop in the absence of a noise photon population, i.e., if somewhere on the $x$ axis $N(x,\tau)$ should vanish. The evolution can not longer transfer photons to this part of the spectrum and the photons accumulate at the lower edge.

## III. EVOLUTION OF AN INTENSE SPECTRUM IN THE PRESENCE OF A CONSTANT NOISE: THE PHOTON SOLITON

To avoid the problem of photon accumulation and in order to look for an universal asymptotic solution independent of the initial spectrum shape, we shall consider first the evolution of a high populated photon spectrum superimposed on a constant noise spectrum $N_0$. The corresponding conservation Eqs. (31) and (32) in this case must be written

$$I_1 = \int_{-\infty}^{+\infty} [N(x,\nu) - N_0]\, dx \equiv N, \tag{33}$$

$$I_2 = \int_{-\infty}^{+\infty} \ln \frac{N(x,\tau)}{N_0}\, dx. \tag{34}$$

We shall see that it is in this case that the nonlinear and nonlocal interaction leads to a downward uniform motion of the spectrum on the frequency axis like a *photon soliton*. Regardless of the explicit form of the solution, if a self-similar solution of $x + v\tau$ exists, we can already give a general expression of the velocity $v$. Substituting $\partial/\partial\tau = v\partial/\partial x$ into Eq. (27) and integrating twice with respect to $x$ (from $-\infty$ to $x$ and from $-\infty$ to $+\infty$), we obtain

$$v = \frac{I_1}{I_2} = \frac{\int_{-\infty}^{+\infty} [N(x,\tau) - N_0]\, dx}{\int_{-\infty}^{+\infty} \ln[N(x,\tau)/N_0]\, dx}. \tag{35}$$

We shall study by a numerical treatment of Eq. (27) the time evolution of several initial spectra. I present here the evolution of a Gaussian spectrum

$$N(x,0) = N_0 + N_1 \exp\{-[(x - x_0)/\delta_0]^2\}, \tag{36}$$

having a narrow ($\delta_0 < 1$) or broad ($\delta_0 > 1$) spectral width, although a large class of other regular spectra—in the presence of a constant noise spectrum $N_0$—leads to the same asymptotic behavior. For simplicity we shall put in the numerical computations

$$N_0 = 1. \tag{37}$$

### A. Evolution of a narrow spectrum of width $\delta_0 \ll 1$

Figure 1 shows the evolution with time of a narrow Gaussian spectrum of width $\delta_0 = \frac{1}{50}$, maximum amplitude $N_1 = 10^8$, and norm $N = \sqrt{\pi}\, \delta_0 (N_1 - N_0) = 3.5449 \times 10^6$. The ordinate is in logarithmic scale. We can see during the first stage of the downward evolution the transformation of the initial spectrum into a red satellite on the spectrum noise $N_0 = 1$. The two different abscissa scales in

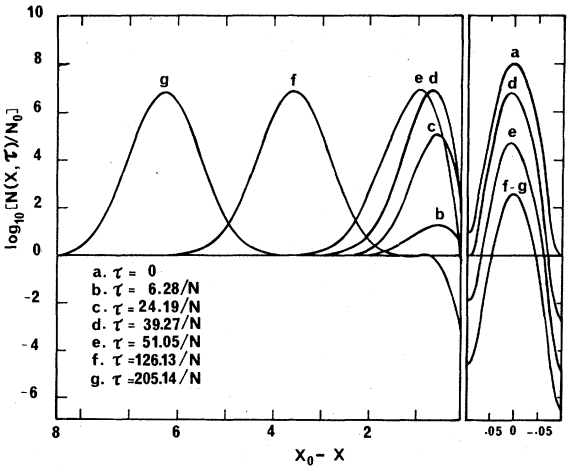


FIG. 1. Nonlinear Compton evolution with time $\tau$ of a narrow Gaussian spectrum (of width $\delta_0 = \frac{1}{50}$, amplitude $N_1\ 10^8$, and norm $N = 3.5449 \times 10^6$) towards a *photon soliton* in the presence of a constant noise $N_0 = 1$. Semilogarithmic scale. Around $x = x_0$ the abscissa is scaled differently in order to visualize the satellization stage.

Fig. 1 allow a better visualization of the satellization stage. The satellite grows at a distance

$$x_0 - x_s \simeq 1/\sqrt{2}\ , \tag{38}$$

where the action of the antisymmetric kernel of Eq. (27) is maximum. Indeed, we can write Eq. (27)

$$\frac{\partial}{\partial t}\ln\left(\frac{N(x,\tau)}{N_0}\right)=\frac{1}{\sqrt{\pi}}\int_{-\infty}^{\infty}dx'\left(\frac{\partial}{\partial x}\exp[-(x-x')^2]\right)\times[N(x',\tau)-N_0]. \tag{39}$$

Introducing for the initial narrow spectrum of form (36) the limit approximation

$$N(x,0)=N_0+\sqrt{\pi}\,\delta_0 N_1\delta(x-x_0)$$

in the right-hand side of Eq. (39), we have, at the initial stage,

$$\frac{\partial}{\partial\tau}\ln\left(\frac{N(x,\tau)}{N_0}\right)=\gamma_0(x)\ , \tag{40}$$

where

$$\gamma_0(x)=\delta_0 N_1\frac{\partial}{\partial x}\exp[-(x-x_0)^2] \tag{41}$$

has a maximum at

$$x_{\max}=x_0-1/\sqrt{2} \tag{42}$$

which will be responsible for the enhancement of the low-frequency side and the formation of the red satellite, and $\gamma_0(x)$ has a minimum on the blue side at $x_{\min}=x_0+1/\sqrt{2}$, where the damping effect is strongest. From (41), the growth rate at $x=x_{\max}$ is given by

$$\gamma_0(x_{\max})=(2/e)^{1/2}\delta_0 N_1\ , \tag{43}$$

and the characteristic time $\tau_{\rm sat}$ for generation of the satellite of width $1/\sqrt{2}$ on the noise spectrum $N_0$ by relaxation of the initial amplitude spectrum $N_1$ of width $\delta_0$ by a factor $1/e$ is given by

$$\tau_{\rm sat}\simeq[\gamma_0(x_m)]^{-1}\left(\ln\frac{N_1}{N_0}-\ln\frac{\delta_0}{e\sqrt{2}}\right)=\left(\ln\frac{N_1}{N_0}-\ln\frac{\delta_0}{e\sqrt{2}}\right)\left(\frac{2}{e}\right)^{1/2}\delta_0 N_1\ . \tag{44}$$

The satellization stage has been described extensively in Refs. 24 and 28 in the presence of a source term for Eq. (27).

While the satellite grows the initial spectrum decreases in order to conserve the norm $N=I_1$, i.e., the total number of photons. Afterwards, the satellite, which now contains the major part of the photon spectrum, moves downward on the frequency $(x)$ axis at constant velocity $v$. It behaves as a *photon soliton* the numerical shape of which is fitted with very great accuracy by the self-similar form

$$\ln\frac{N(x,\tau)}{N_0}=\left(\ln\frac{N_m}{N_0}\right)\exp[-(x-x_0+v\tau)^2]\ , \tag{45}$$

where $N_m$ is the maximum amplitude corresponding to abscissa

$$x_m(\tau)=x_0-v\tau\ . \tag{46}$$

In fact, (45) is an exact asymptotic form of Eq. (27) or (39) for $N_m/N_0\to\infty$. The velocity $v=|dx_m/d\tau|$ can be obtained easily if we substitute the spectrum entering the integrant in the right-hand side of Eq. (39) by its form as given in (45), namely,

$$N(x,\tau)=N_0\exp\{\ln(N_m/N_0)\times\exp[-(x-x_0+v\tau)^2]\}\ . \tag{47}$$

Indeed, since $\ln(N_m/N_0)\gg 1$, we can expand (47) as

$$N(x,\tau)\simeq N_0\exp\{\ln(N_m/N_0)[1-(x-x_0+v\tau)^2]\}\ ,$$

and, setting the correct dependence on the noise $N_0$ for $x-x_0+v\tau=0$ and for $x\to\pm\infty$, according to (47), get

$$N(x,\tau)-N_0=(N_m-N_0)\exp[-\ln(N_m/N_0)\times(x-x_0+v\tau)^2]\ . \tag{48}$$

The narrowness of the soliton profile—its width

$$\delta_s=[\ln(N_m/N_0)]^{-1/2} \tag{49}$$

is smaller by the same factor $\delta_s$ than the unity width of the Gaussian transition-probability kernel—allows us to introduce the limit expression of (48),

$$N(x,\tau)-N_0\to\frac{\sqrt{\pi}\,(N_m-N_0)}{[\ln(N_m/N_0)]^{1/2}}\delta(x-x_0+v\tau)\ , \tag{50}$$

into the integrand of Eq. (39), and integrating over $x'$, we obtain

$$\frac{\partial}{\partial\tau}\ln\left(\frac{N(x,\tau)}{N_0}\right)=\frac{N_m-N_0}{[\ln(N_m/N_0)]^{1/2}}\frac{\partial}{\partial x}\times\exp[-(x-x_0+v\tau)^2]\ . \tag{51}$$

By taking into account the soliton form (45), this may be written as an equation of linear uniform motion in the $x$ axis

$$\frac{\partial}{\partial\tau}\ln\left(\frac{N(x,\tau)}{N_0}\right)=v\frac{\partial}{\partial x}\ln\left(\frac{N(x,\tau)}{N_0}\right), \tag{52}$$

where the soliton velocity is given by

$$v=(N_m-N_0)/[\ln(N_m/N_0)]^{3/2}\ . \tag{53}$$

This formula could also be obtained from the general expression (35), since from (48) and (45) we have

$$I_1=\sqrt{\pi}\,(N_m-N_0)/[\ln(N_m/N_0)]^{1/2}\ , \tag{54}$$

$$I_2 = \sqrt{\pi}\,\ln(N_m/N_0)\,, \tag{55}$$

and (53) follows from (35). Expression (53) for the soliton velocity agrees very well with the numerical value $\Delta x_m/\Delta\tau$, namely,

$$\Delta x_m/\Delta\tau = 1.2113\times10^5$$
$$v = (N_m - N_0)/[\ln(N_m/N_0)]^{3/2}$$
$$= 1.2030\times10^5\,,$$

a discrepancy of less than 1%. The agreement increases with increasing values of $N_m/N_0$; here $N_m/N_0 = 7.5857\times10^6$.

Equation (51) has the same form as Eq. (41), where $\gamma_0(x)$ is here

$$\gamma(x) = \frac{N_m - N_0}{[\ln(N_m/N_0)]^{1/2}}\,\frac{\partial}{\partial x}\,\exp[-(x-x_m)^2]\,, \tag{56}$$

$x_m$ being given by (46). It has therefore the two extrema

$$x_{\max} = x_m - 1/\sqrt{2}\quad, \tag{57}$$

$$x_{\min} = x_m + 1/\sqrt{2}\quad. \tag{58}$$

Now, however, the enhancement is maximum on the proper red wing of the spectrum and an antisymmetrical damping is exerted on the blue wing. The resulting action is the uniform motion of the spectrum as a soliton.

In a different way, we can directly obtain the soliton form (45) and its velocity expression (53) from general arguments about the narrowness of the soliton profile with respect to the kernel's width. Indeed, we first take for the narrow spectrum entering the right-hand side of Eq. (39) the limit approximation

$$N(x,\tau) - N_0 = \sqrt{\pi}\,A\delta(x - x_0 + v\tau)\,, \tag{59}$$

whose norm

$$I_1 = \int_{-\infty}^{+\infty}[N(x,\tau) - N_0]\,dx = \sqrt{\pi}\,A \tag{60}$$

is conserved, $A$ being a constant. Therefore

$$\frac{\partial}{\partial\tau}\ln\left(\frac{N(x,\tau)}{N_0}\right) = A\,\frac{\partial}{\partial x}\,\exp[-(x-x_0+v\tau)^2]$$
$$= \frac{A}{v}\,\frac{\partial}{\partial\tau}\,\exp[-(x-x_0+v\tau)^2]\,, \tag{61}$$

and, integrating with respect to time, we have

$$\ln[N(x,\tau)/N_0] = (A/v)\exp[(x-x_0+v\tau)^2]\,, \tag{62}$$

$$N(x,\tau)/N_0 = \exp\{(A/v)\exp[-(x-x_0+v\tau)^2]\}\,. \tag{63}$$

Assuming *a priori* $A/v \gg 1$, we may develop (63) and obtain a second approximation for the spectrum

$$N(x,\tau) - N_0 = N_0[\exp(A/v) - 1]$$
$$\times\exp[-(A/v)(x - x_0 + v\tau)^2]\,, \tag{64}$$

where the maximum amplitude turns to be

$$N_m = N_0\exp(A/v)\,. \tag{65}$$

Therefore

$$A/v = \ln(N_m/N_0)\,; \tag{66}$$

substituting this expression into (62), we again obtain the same form (45). The velocity $v$ in (62) will be determined by the general formula (35): from (64) and (62) and taking into account (66), we obtain the same values (54) and (55) for the invariants $I_1$ and $I_2$ and therefore from (35) follows, too, the same expression (53) for $v$. As can be seen in Fig. 1, the soliton has collected the major part of the initial spectrum norm. It has left however a small-amplitude spectrum around $x = x_0$. In its downward motion, the first soliton increases the distance between itself and the initial spectrum and becomes uncorrelated with it. In a much longer characteristic time—proportional to its amplitude—this small spectrum (of amplitude $N_{m,2}/N_0 \simeq 320$) will also evolve downward on the $x$ axis. In other words, the nonlinear and nonlocal action of the kernel in Eq. (27) first transfers by satellization almost all the initial spectrum to the first soliton and will afterward repeat this action with the residual spectrum.

### B. Evolution of a broad spectrum of width $\delta_0 \gg 1$

As I said in the Introduction, induced Compton scattering of a broad electromagnetic spectrum has been described up to now by the Kompaneets differential equation (5), which corresponds to the $\delta'(x-x')$ approximation of the complete kernel $\partial_x\exp[-(x-x')^2]$ of Eq. (27). The absence of a dispersive term—this term would be present if the kernel is developed up to $\delta'''(x-x')$ as in Eq. (8)—forestalls formation of the fine soliton structure. I therefore describe broad spectral evolution by means of the complete master equation (27). Figure 2 shows the numerical evolution of a broad Gaussian spectrum (36) with initial amplitude $N_1 = 10^8$, width $\delta_0 = 7.5$, and norm $N = \sqrt{\pi}\,\delta_0(N_1 - N_0) = 1.3293\times10^9$. During the initial stage ($0 < \tau < 1.39/N$) we can see the whole triangular distortion of the spectrum, the shift of its maximum towards lower frequencies, and the

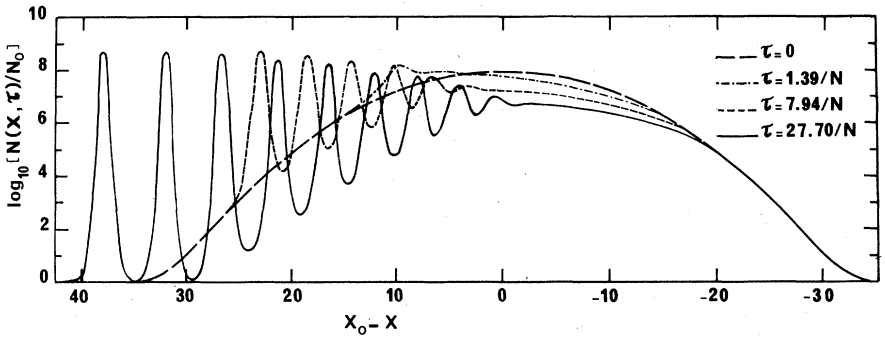


FIG. 2. Nonlinear Compton evolution with time $\tau$ of a broad Gaussian spectrum (of width $\delta_0 = 7.5$, amplitude $N_1 = 10^8$ and norm $N = 1.3293 \times 10^9$) giving rise to a set of *photon solitons*. Semilogarithmic scale. Constant noise $N_0 = 1$.

steepening of its red side. Up to this point this could be qualitatively described by Eq. (5), since the differential distortion of the spectrum is proportional to the spectral amplitude $N(x,\tau)$, which plays the role of a speed for the maximum amplitude. Then, however, the general evolution governed by Eq. (27) begins to be dispersive and cannot be described by Eq. (5). Indeed, the spectrum sinks behind the maximum, generating another peak due to the nonlocal action of the kernel. In the following stages, the spectrum is broken completely into secondary ones which move downwards on the $x$ axis, approaching more and more closely the photon soliton form (45) or (47) when they leave the initial spectrum and propagate on the constant noise spectrum. The number of photon solitons generated is proportional to the norm $N$, as is common to other nonlinear equations leading to multisoliton solutions. In their motion downward on the frequency axis they are ordered by their amplitudes or, equivalently, by their speeds, therefore increasing the distances between them.

### C. Summary

Numerical computation of Eq. (27) shows that, in the presence of a constant noise spectrum $N_0$, the initial high populated photon spectrum—narrow or broad—evolves, after a transient regime, by a *uniform* nonlinear and nonlocal coupling with the *uniform* noise $N_0$, towards a soliton or a set of solitons (this name being understood in the sense of Makhankov[33]; cf. the end of Sec. I). This asymptotic solution of Eq. (27) is fitted very well by expression (45), which is a self-similar form depending on $x + v\tau$ and on the constant noise $N_0$.

## IV. EVOLUTION OF AN INTENSE SPECTRUM IN THE ABSENCE OF A CONSTANT NOISE SPECTRUM

Of course, in the absence of a constant noise spectrum $N_0$, the solution of Eq. (27) cannot take the self-similar soliton form (45), which has been constructed over $N_0$ and depends on $N_0$. Starting with a high-amplitude spectrum ($N \gg 1$) centered at $x = x_0$ and decreasing to zero as $x \to \pm\infty$ according to some law, we must look for self-similar solutions which suit the $x$-dependent law of the initial spectrum shape. Before looking for such analytical approximations we shall present the results of the numerical computation of Eq. (27).

Figure 3 shows the time evolution of a narrow Gaussian spectrum of width $\delta_0 = 1/4\sqrt{2}$, maximum amplitude $N_1 = 10^6$, and norm $N = 3.13332 \times 10^5$ in the absence of any noise spectrum, i.e., $N_0 = 0$ in expression (36). As emphasized in Sec. I, contrarily to the result obtained within the $x - x'$ local approximation for the kernel,[14] the narrow

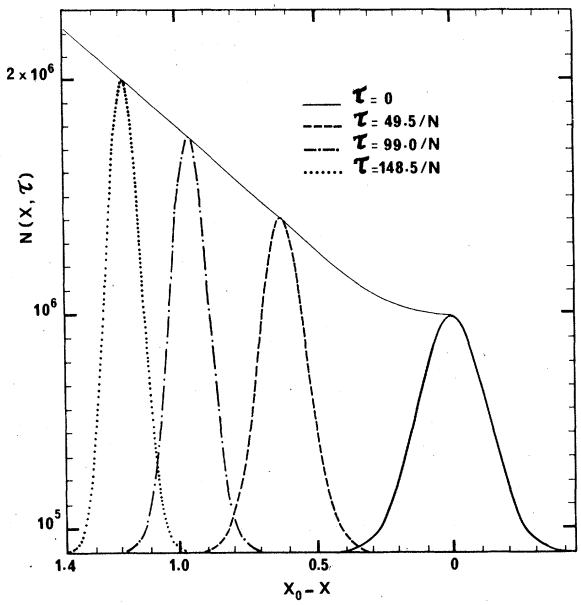


FIG. 3. Nonlinear Compton evolution with time $\tau$ of a narrow Gaussian spectrum (of width $\delta_0 = \frac{1}{4}\sqrt{2}$, amplitude $N_1 = 10^6$, and norm $N = 3.1332 \times 10^5$) in the absence of a constant noise spectrum. Natural scale. The thin line enveloping the maxima shows the linear dependence of the amplitude on the shift $x_0 - x_m(\tau)$.

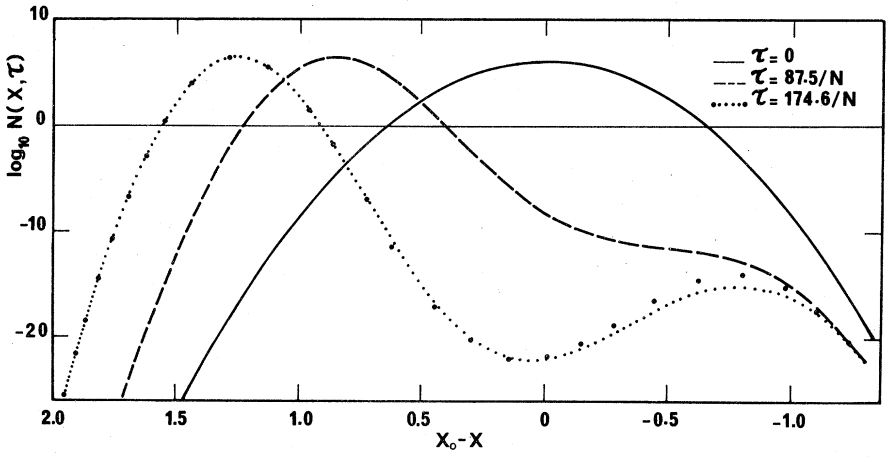


FIG. 4. Same time evolution as in Fig. 3, but in semilogarithmic scale and for different time parameters $\tau$. The logarithmic scale shows better the detailed spectral form, in particular the appearance of a second bump on the low tail end. For time $\tau = 174.6/N$ the theoretical curve obtained from Eq. (93) and marked with heavy dots shows a good fitting of the numerical curve (small dots) except for a discrepancy on the small tail end.

Gaussian spectrum does not maintain its form during its downward motion on the frequency axis. Indeed, its amplitude grows and its profile becomes narrower and asymmetric while its speed decreases. It seems like a solitary spectrum moving on a decreasing-amplitude "noise" which is nothing else than its own low-frequency wing. This is visualized better in Fig. 4, which shows the time evolution for the same initial spectrum in logarithmic scale. The logarithmic dependence of soliton (45) on the noise $N_0$ turns to be here a logarithmic response on the $x$-dependent wing amplitude, as if the moving spectrum bump fits the decreasing wing adiabatically. We see in Fig. 3 that during its downward motion, the amplitude of the solitary spectrum increases linearly with $x_0 - x$ as soon as $|x - x_0| > \delta_0$, while its width narrows by approximately the same linear rate in order to conserve the norm. One might infer this from expression (49) assuming $N_0 \propto N_1 \exp\{-[(x - x_0)/\delta_0]^2\}$. However, in order to look for an analytical self-similar form of $(x,\tau)$ which tries to fit the spectral evolution with time plotted on Figs. 3 and 4, let us generalize the method used in Sec. III by introducing a time-dependent velocity

$$v(\tau) = |dx_m(\tau)/d\tau| = \dot{g}(\tau) \tag{67}$$

for the downward motion of $N(x,\tau)$ so that

$$g(\tau) = \int_0^\tau v(\tau')d\tau' \geq 0 \ . \tag{68}$$

The narrowness of the initial spectrum allows us to introduce the approximate form

$$N(x,\tau) = N[x_m(\tau)] \exp\left\{-\left[\left(x - x_0 + \int_0^\tau v(\tau')d\tau'\right)\Big/\delta_0(\tau)\right]^2\right\} \sim \sqrt{\pi}\,\delta_0(\tau) N[x_m(\tau)]\,\delta\left(x - x_0 + \int_0^\tau v(\tau')d\tau'\right), \tag{69}$$

whose norm

$$I_1 = \int_{-\infty}^{\infty} N(x,\tau)dx$$

$$= \sqrt{\pi}\,\delta_0(\tau) N[x_m(\tau)] = \sqrt{\pi}\,\delta_0 N_1 = \sqrt{\pi}\,A \tag{70}$$

is conserved, into the integrand of Eq. (27), and, integrating with respect to time, we have

$$\ln N(x,\tau) = A\int_0^\tau \frac{\partial}{\partial x} \exp\{-[x - x_0 + g(\tau')]^2\}d\tau' - \ln N(x,0)$$

$$= A\int_0^\tau \frac{1}{\dot{g}} \frac{\partial}{\partial \tau'} \exp\{-[x - x_0 + g(\tau')]^2\}d\tau' - \ln N(x,0), \tag{71}$$

Therefore

$$\ln \frac{N(x,\tau)}{N(x,0)} = A\left(\frac{1}{\dot{g}} \exp\{-[x - x_0 + g(\tau)]^2\}\right)_0^\tau + A\int_0^\tau \frac{\ddot{g}}{\dot{g}^2} \exp\{-[x - x_0 + g(\tau')]^2\}d\tau', \tag{72}$$

and setting $\dot{g}(0)=g_0$, $g(0)=0$ from (68) and $d\tau'=d\tilde{g}/\dot{g}$, we can write

$$\ln\frac{N(x,\tau)}{N(x,0)}=A\left(\frac{1}{\dot{g}}\exp[-(x-x_0+g)^2]-\frac{1}{\dot{g}_0}\exp[-(x-x_0)^2]\right)+A\int_0^g\frac{\dddot{\tilde{g}}}{\dot{\tilde{g}}^3}\exp[-(x-x_0+\tilde{g})^2]d\tilde{g}\ , \tag{73}$$

where integration is over the dumb variable $\tilde{g}$. Now we may set for $N(x,0)$ the initial Gaussian spectrum of amplitude $N_1$ and width $\delta_0$. Thus the spectrum takes the form

$$N(x,\tau)=N_1\exp\left(-\frac{(x-x_0)^2}{\delta_0^2}+\frac{A}{\dot{g}}\exp[-(x-x_0+g)^2]-\frac{A}{\dot{g}}\exp[-(x-x_0)^2]+A\int_0^g\frac{\dddot{\tilde{g}}}{\dot{\tilde{g}}^3}\exp[-(x-x_0+\tilde{g})^2]d\tilde{g}\right), \tag{74}$$

where the function $g=g(\tau)$ will be determined by imposing the norm conservation equation (70), as we shall see.

During the first transient stage, the spectrum shifts towards lower $x$ and is at the same time dissymmetrized or distorted (cf. Figs. 3 and 4). It is easy to show that for a Gaussian profile the two effects act with the same characteristic time. Indeed, on the one hand, replacing $N_0$ from (44) by the Gaussian wing amplitude at $x_m=x_0-1/\sqrt{2}$,

$$N(x=x_m,0)=N_1\exp(-2/\delta_0^2)\ , \tag{75}$$

we obtain the characteristic distortion time, from (44),

$$\tau_{\text{dist}}\simeq\left(\frac{2}{\delta_0^2}-\ln\frac{\delta_0}{e\sqrt{2}}\right)\Big/\left(\frac{2}{e}\right)^{1/2}\delta_0N_1\propto(\delta_0^3N_1)^{-1}. \tag{76}$$

On the other hand, during the first stage, when $g(\tau)$ begins to take small but finite values in (74) we may assume

$$g\simeq\dot{g}_0\tau\ll 1\ , \tag{77}$$

$$A/\dot{g}\simeq A/\dot{g}_0\gg 1\ , \tag{78}$$

and, neglecting the last term in the right-hand side of (74), we develop this expression as follows:

$$N(x,\tau)\simeq N_1\left(-\frac{(x-x_0)^2}{\delta_0^2}-2A[(x-x_0)\tau+\dot{g}_0\tau^2]\right)$$
$$=N_1\exp\left[-\left(\frac{x-x_0+\dot{g}_0\tau}{\delta_0}\right)^2\right], \tag{79}$$

with the initial velocity defined by

$$\dot{g}_0=A\delta_0^2=N_1\delta_0^3\ , \tag{80}$$

which yields a characteristic time of the same order as (76) does for distorting.

Now let us determine $g=g(\tau)$ in (74) from the norm conservation equation (70). After the transient stage and because of the great value for $A/\dot{g}$, the solitary spectrum have a peak around

$$x_m(\tau)=x_0-g(\tau)\ , \tag{81}$$

in analogy with the soliton case, where $g=v\tau$ [cf. (46)]. Thus we can evaluate Eq. (70) by the "steepest-descent method" applied to maximum (81). With the exponent function in (74) defined by

$$\varphi(x,\tau)=\ln[N(x,\tau)/N_1]\ , \tag{82}$$

Eq. (70) yields

$$I_1=\sqrt{\pi}\ A=\sqrt{\pi}\ \delta_0N_1$$
$$=\sqrt{\pi}\ \delta_0(\tau)N_1\exp\{\ln[\delta_0/\delta_0(\tau)]\}$$
$$\simeq\int_{-\infty}^{\infty}N_1\exp[\varphi(x_m)+\tfrac{1}{2}\varphi''(x_m)(x-x_0+g)^2]dx\ , \tag{83}$$

where the prime stands for derivation with respect to $x$ and

$$\varphi(x_m)\equiv-\frac{g^2}{\delta_0^2}+\frac{A}{\dot{g}}-\frac{A}{\dot{g}_0}\exp(-g^2)$$
$$+A\int_0^g\frac{\dddot{\tilde{g}}}{\dot{\tilde{g}}^3}\exp[-(\tilde{g}-g)^2]d\tilde{g}$$
$$=\ln[\delta_0/\delta_0(\tau)]\ , \tag{84}$$

$\delta_0(\tau)$ being the width of the solitary spectrum,

$$\delta_0(\tau)=[-\tfrac{1}{2}\varphi''(x_m)]^{-1/2}\ , \tag{85}$$

which will be evaluated later from a more tractable form of $\varphi(x,\tau)$ than (74). Nevertheless, taking into account the approximate expansion (83), we directly obtain from (74) a correct order-of-magnitude estimate for $\delta_0(\tau)$:

$$\delta_0(\tau)\simeq(\dot{g}/A)^{1/2}\ . \tag{86}$$

Introducing this expression into the right-hand side of Eq. (84), we obtain a self-consistent equation $f(g, \dot{g}, \ddot{g}) = 0$, the solution of which determines $g = g(\tau)$ and therefore, from (74), the explicit spectral dependence $N(x, \tau)$. Equation (84), however, is complicated and will be solved in the Appendix by successive approximations ($g \gg 1$) yielding the following third-order algebraic equation:

$$\tau = (1/3\delta_0^2 A)[g^3 + \tfrac{1}{2}3\sqrt{\pi}\, g^2 + 3(\tfrac{1}{2}\pi - 1)g + K], \quad (87)$$

for which the solution $g = g(\tau)$ is standard. With a convenient choice of the constant $K$, the solution $g(\tau)$ so obtained fits with good accuracy, when $g(\tau) \gg 1$, the abscissa $x_m(\tau) = x_0 - g(\tau)$ of the main spectral maximum evaluated by numerical computation. Even if we are not in the full asymptotic regime ($3\delta_0^2 A\tau \gg 1$, $g \gg 1$) but only satisfy $g \gtrsim 1$, for the last spectral bumps in Figs. 3 and 4, the parameter $K$ remains almost constant in Eq. (87), with $\Delta K/K < 3.6\%$ (see Table I).

Time derivation of Eq. (87) yields

$$\dot{g}/A = \delta_0^2/(g^2 + \sqrt{\pi}\, g + \tfrac{1}{2}\pi - 1), \quad (88)$$

$$A\ddot{g}/\dot{g}^3 = -(1/\delta_0^2)(2g + \sqrt{\pi}), \quad (89)$$

which are useful formulas. Indeed, (88) allow us to compare the width $\delta_0(\tau)$ given by the approximate expression (86) with the result of the numerical computation. For the above values (Table I) we have, as shown in Table II, a discrepancy of less than $6^0/_{00}$.

Moreover, in the full asymptotic regime ($3\delta_0^2 A\tau \gg 1$, $g \gg 1$), $\delta_0/(g/A)^{1/2}$ has a linear dependence on $g(\tau) = x_0 - x_m(\tau)$ which corresponds by virtue of norm conservation equation (83) to a linear growth of the amplitude $N[x_m(\tau)]$ with respect to $x_0 - x_m(\tau)$. The thin line enveloping the maxima in Fig. 3 shows this linear dependence. In the same asymptotic regime we have from (87)

$$g \simeq (3\delta_0^2 A\tau)^{1/3}, \quad (90)$$

and, differentiating with respect to $\tau$, or from (88),

$$v = \dot{g} \simeq A\delta_0^2/g^2 \simeq (\delta_0^2 A)^{1/3}(3\tau)^{-2/3}, \quad (91)$$

the logarithmic form of which,

$$\ln v = \text{const} - \alpha \ln \tau, \quad \alpha = \tfrac{2}{3},$$

agrees with the numerical computation, since we obtain $\alpha = 0.648$. From (91) and (81) we obtain the following dependence with respect to $x_0 - x_m(\tau)$:

$$v(\tau) \simeq A\delta_0^2[x_0 - x_m(\tau)]^{-2}, \quad (92)$$

which could be expected from expression (53), as has been said, by assuming $N_m \propto (x_0 - x_m)$, $N_0 \propto N_1 \exp[-(x_0 - x_m)^2]$.

Introducing Eqs. (88) and (89) into (74), we obtain the explicit spectral form $N(x, \tau)$, which will be compared to the numerical evolutions of Figs. 3 and 4. First of all, (89) allow us to modify the integrand in (74) in order to obtain a simpler expression for $\varphi(x, \tau)$, namely,

$$\varphi(x,\tau) = \ln[N(x,\tau)/N_1]$$
$$= -\frac{(x-x_0)^2}{\delta_0^2} + \left(\frac{A}{\dot{g}} + \frac{1}{\delta_0^2}\right)\exp[-(x - x_0 + g)^2] - \left(\frac{A}{\dot{g}_0} + \frac{1}{\delta_0^2}\right)\exp[-(x-x_0)^2] + \frac{2}{\delta_0^2}(x - x_0 - \tfrac{1}{2}\sqrt{\pi})$$
$$\times \int_0^g \exp[-(x - x_0 + \bar{g})^2]\, d\bar{g}, \quad (93)$$

where $A/\dot{g}$ is given by (88) and $A/\dot{g}_0$ is the initial value. Even if (88) is obtained within the asymptotic limit $g \gg 1$, a good order-of-magnitude estimate for $A/\dot{g}_0$ is obtained from (88) by setting $g(\tau = 0) = 0$, i.e.,

$$A/\dot{g}_0 = (\tfrac{1}{2}\pi - 1)/\delta_0^2 = 18.26. \quad (94)$$

However, we shall obtain a better determination of

TABLE I. Comparison of values for parameters $\tau N$, $\delta(\tau)$, and $K$ found for the last spectral bumps in Figs. 3 and 4.

| | Numerical computation | | Eq. (86) |
|---|---|---|---|
| | $\tau N$ | $g(\tau) = x_0 - x_m(\tau)$ | $K$ |
| Fig. 3 | 148.5 | 1.184 | 0.439 |
| Fig. 4 | 174.6 | 1.290 | 0.455 |

TABLE II. Comparison of parameter values found by numerical computation and with Eq. (88) for the last spectral bumps in Figs. 3 and 4.

| | Numerical computation | | Eq. (88) |
|---|---|---|---|
| | $g(\tau) = x_0 - x_m(\tau)$ | $\delta_0/\delta_0(\tau)$ | $\delta_0/(\dot{g}/A)^{1/2}$ |
| Fig. 3 | 1.184 | 2.028 | 2.017 |
| Fig. 4 | 1.290 | 2.138 | 2.126 |

the parameter $A/\dot{g}_0$ in (93) by adjusting the maximum amplitude $N[x_m = x_0 - g(\tau)]$ obtained from numerical computation to that obtained from (93). Expression (93), more precisely $\ln N(x,\tau) = \varphi(x,\tau) - \ln N_1$, is represented in Fig. 4 for time $\tau = 174.6/N$ and, as we can see, shows an excellent agreement with the numerical curve except for a small discrepancy on the small tail end. We have taken $A/\dot{g} = 22$. Neither this value nor (94) coincides with (80); i.e., the velocity of the solitary spectrum at the beginning of the asymptotic regime, governed by Eqs. (87)–(89), differs from that of the initial transient stage. This transient stage corresponds to the inflection of the thin line enveloping the maxima in Fig. 3 where the velocity first increases before attaining regime (88) or (91).

From (93) we can obtain analytical expressions for the characteristic points of the curve. In particular, we give here the result of $\varphi'(x,\tau)$ in the neighborhood of $x = x_0 - g(\tau)$ in order to justify the approximate expression (81). Thus

$$\varphi'(x,\tau) \simeq 2(x - x_0)\left(-\frac{1}{\delta_0^2} - \frac{A}{\dot{g}} + \frac{A}{\dot{g}_0}\exp(-g^2)\right) - 2g\left(\frac{A}{\dot{g}} + \frac{1}{\delta_0^2}\right) + \frac{\sqrt{\pi}}{\delta_0^2}\exp(-g^2), \tag{95}$$

and, setting $\varphi'(x,\tau) = 0$, we obtain

$$x_m - x_0 = \frac{[g(A/\dot{g} + 1/\delta_0^2) - (\sqrt{\pi}/2)(1/\delta_0^2)\exp(-g^2)]}{[-A/\dot{g} - 1/\delta_0^2 + (A/\dot{g}_0)\exp(-g^2)]} \simeq -g \quad (g \gg 1). \tag{96}$$

Even for the value $g = 1.290$ in Tables I and II we obtain an excellent agreement: $x_0 - x_m = 1.292$.

We can finally evaluate $\varphi''(x,\tau)$ from (93) at $x = x_0 - g(\tau)$ in order to test expression (86), taking (85) into account. We have

$$[\varphi''(x,\tau)]_{x=x_m} = -\frac{2}{\delta_0^2(\tau)} = -\frac{2A}{\dot{g}} + 2\left(\frac{A}{\dot{g}_0}(1 - 2g^2) + \frac{\sqrt{\pi}}{\delta_0^2}g - \frac{1}{\delta_0^2}\right)\exp(-g^2), \tag{97}$$

which leads to (86) for $g \gg 1$. In Table III this more precise width (97) is compared with the values of Table II, with a resulting relative discrepancy of less than $4\times10^{-4}$.

## V. COMPARISON WITH LOCAL APPROXIMATION

The $x - x'$ local approximation for the kernel in Eq. (27), already discussed in Sec. I, leads to the equation

$$\frac{\partial N(x,\tau)}{\partial \tau} = \frac{2N(x,\tau)}{\sqrt{\pi}}\int_{-\infty}^{\infty} dx'(x - x')N(x',\tau), \tag{98}$$

the formal solution of which is given by[14]

$$N(x,\tau) = N(x,0)\exp\left(\frac{2}{\sqrt{\pi}}\int_0^\tau d\tau' \int_{-\infty}^{\infty} dx'\, x' N(x',\tau) - \frac{2x}{\sqrt{\pi}}N\tau\right), \tag{99}$$

where $N = \sqrt{\pi}A$ is the norm. For an initial narrow Gaussian spectrum of width $\delta_0 \ll 1$, centered at $x = x_0$, we can write

$$N(x,\tau) = N_1 \exp\{-[(x - x_0 + v\tau)/\delta_0]^2\}\Psi(\tau), \tag{100}$$

where

$$v = N\delta_0^2/\sqrt{\pi} = A\delta_0^2, \tag{101}$$

and

$$\Psi(\tau) = \exp\left[-\frac{2x_0 v\tau}{\delta_0^2} + \left(\frac{v\tau}{\delta_0}\right)^2\right] \times \exp\left(\int_0^\tau d\tau' \int_{-\infty}^{\infty} dx'\, x' N(x',\tau')\right) \tag{102}$$

is an independent function of $x$. Conservation of the norm, however,

$$N = \int_{-\infty}^{\infty} N(x',\tau')dx' = \sqrt{\pi}\,\delta_0 N_1 \Psi(\tau) \tag{103}$$

yields

$$\Psi(\tau) = \text{const}. \tag{104}$$

Therefore, within the local approximation used by Zel'dovich *et al.*,[14] the initial narrow Gaussian spectrum cannot be distorted, contrary to the general result of Sec. IV. It only admits a uniform shift towards lower frequencies with velocity (101), which is nothing more than the velocity (80) of the initial transient stage.

## VI. CONCLUSION

We have seen that induced Compton scattering of a high populated photon spectrum governed by the integral equation (27) leads to different qualitative evolutions depending upon the presence or

TABLE III. Comparison of parameter values found by numerical computation and with Eq. (97) for the last spectral bumps of Figs. 3 and 4.

| | Numerical computation | | Eq. (97) |
|---|---|---|---|
| | $g(\tau) = x_0 - x_m(\tau)$ | $\delta_0/\delta_0(\tau)$ | $\delta_0[\frac{1}{2}\varphi''(x_m)]^{1/2}$ |
| Fig. 3 | 1.184 | 2.028 | 2.025 |
| Fig. 4 | 1.290 | 2.138 | 2.139 |

absence of a constant noise spectrum $N_0$. In the first case ($N_0 > 0$) a large class of initial spectra give rise to universal solitonlike structures which move downward on the frequency axis with uniform motion (Sec. III). In the absence of a constant noise ($N_0 = 0$), the downward motion of the solitary spectrum depends at each time on the form of the initial spectrum profile (Sec IV). Thus the downward motion of a narrow Gaussian spectrum is accompanied by an increasing of its maximum amplitude, a narrowing of its width and a diminution of its velocity. However, in physical situations it is difficult to assume the total absence of a noise spectrum. So, for the narrow Gaussian profile of width $\delta_0 = 1/4\sqrt{2}$ and initial amplitude $N_1 = 10^6$, studied in Sec. IV, the amplitude of the low-frequency wing becomes extremely low for Doppler-Compton distances $x_0 - x > 1$, i.e.,

$$N(x_0 - x = 1.0) = 1.26 \times 10^{-8},$$

$$N(x_0 - x = 1.29) = 7.47 \times 10^{-18},$$

$$N(x_0 - x = 2.0) = 2.57 \times 10^{-50}.$$

Thus even an extremely small white noise would change the nonlinear evolution to the solitonlike case.

The asymptotic analysis carried out in Sec. IV for an initial Gaussian profile may be generalized to the more general form

$$N(x, 0) = N_1 \exp\{-(x - x_0)^2/\delta_0^2[1 + \epsilon(x - x_0)^2]\}, \quad (105)$$

which behaves as a Gaussian function for $\epsilon \ll (x - x_0)^2$ and tends to a constant spectrum for $\epsilon \gg (x - x_0)^2$. The corresponding Eq. (84) yields here

$$-\frac{g^2}{\delta_0^2(1 + \epsilon g^2)} + \frac{A}{\dot{g}} - \frac{A}{\dot{g}_0}\exp(-g^2) + A\int_0^g \frac{\dddot{\tilde{g}}}{\dot{\tilde{g}}^3}\exp[-(\tilde{g} - g)^2]d\tilde{g} = 0. \quad (106)$$

Within the limit approximation $g \gg 1$, the treatment developed in the Appendix leads to equation

$$\dot{g}g^2/\delta_0^2(1 + \epsilon g^2) - A(1 + \tfrac{1}{2}\sqrt{\pi}\,\ddot{g}/\dot{g}^2) = 0, \quad (107)$$

integration of which yields

$$\frac{1}{\epsilon^{3/2}\delta_0^2}(\arctan\sqrt{\epsilon}\,g - \sqrt{\epsilon}\,g) + A\left(\tau - \frac{\sqrt{\pi}}{2}\frac{1}{\dot{g}}\right) = C_1; \quad (108)$$

in the limit $\sqrt{\epsilon}\,g \gg 1$, we have

$$-g + \frac{1}{\sqrt{\epsilon}}\frac{\pi}{2} + \epsilon\delta_0^2(A\tau - C_1) = \epsilon\delta_0^2 A\frac{\sqrt{\pi}}{2}\frac{1}{\dot{g}}. \quad (109)$$

Integrating once more, we obtain

$$g = g_0 + v\tau, \quad (110)$$

where $v = \epsilon\delta_0^2 A$ is the expected soliton velocity.

As I have said, the integral equation (27) does not seem to be an exactly integrable equation in spite of the strong structural stability of their solitonlike solutions, which has been tested by studying collisions between them.[32]

Inclusion of the linear terms of Eq. (1) will lead to a dissipation of the soliton structures. One-dimensional models including a small linear dissipative term lead to "quasisolitons"[31,34] or hybrid spectral profiles constituted each by a high-amplitude, exponentially damped solitary pulse together with a small-amplitude shelf leading behind it.

However, inclusion of the linear terms renders the induced Compton scattering problem multidimensional in a real physical case. This general complicated case will be the object of future research.


## ACKNOWLEDGMENTS

I express my gratitude to Dr. J. Peyraud for his interest in this problem. I thank also Dr. J. Coste, Dr. J. C. Fernandez, Dr. M. Hénon, and Dr. G. Reinisch for helpful discussions. The author was a member of the GRECO "Interaction Laser Matière" of the C.N.R.S. when this work was done.


## APPENDIX

We shall solve Eq. (84) by successive approximations: (i) Assuming $g \gg 1$, we evaluate the integral expression in (84) as follows:

$$J \equiv A\int_0^g \frac{\dddot{\tilde{g}}}{\dot{\tilde{g}}^3}\exp[-(\tilde{g} - g)^2]d\tilde{g} \simeq A\frac{\ddot{g}}{\dot{g}^3}\int_0^g \exp(-\tilde{g}^2)d\tilde{g} = \frac{\sqrt{\pi}A}{2}\frac{\ddot{g}}{\dot{g}^3}\operatorname{erf} g. \quad (A1)$$

In the limit $g \to \infty$, we obtain

$$J^{(1)} = \tfrac{1}{2}\sqrt{\pi}\,A\ddot{g}/\dot{g}^3. \quad (A2)$$

[Note that even for not-too-great values of $g$ the approximation is correct. Indeed, $\operatorname{erf}(g = 1.290) = 0.931\,89$]

(ii) The right-hand side of Eq. (84) exhibits a logarithmic dependence:

$$\ln[\delta_0/\delta_0(\tau)] \simeq \ln[\delta_0(A/\dot{g})^{1/2}]. \quad (A3)$$

We shall see [cf. (91)] that $\delta_0(A/\dot{g})^{1/2} \simeq g$ for $g \gg 1$ and (A3) may be neglected in Eq. (84).

Therefore we are led in a first step to solve the approximate equation

$$\frac{g^2}{\delta_0^2} + \frac{A}{\dot{g}_0}\exp(-g^2) = \frac{A}{\dot{g}}\left(1 + \frac{\sqrt{\pi}}{2}\frac{\ddot{g}}{\dot{g}^2}\right), \quad (A4)$$

otherwise written

$$\frac{dg^3}{3\delta_0^3} + \frac{A}{\dot{g}_0}\exp(-g^2)dg = A\left(1 + \frac{\sqrt{\pi}}{2}\frac{\ddot{g}}{\dot{g}^2}\right)d\tau,$$

integration of which in the limit $g(\tau) \gg 1$, assuming $g(\tau = 0) = 0$, yields

$$\frac{g^3}{3\delta_0^3} + \frac{\sqrt{\pi}}{2}\frac{A}{\dot{g}} - A\tau = C_1 . \tag{A5}$$

Let us write (A5) as

$$\frac{d\tau}{dg} - \frac{2}{\sqrt{\pi}}\tau = -\frac{2}{3\sqrt{\pi}\,\delta_0^2 A}(g^3 - 3\delta_0^2 C_1) , \tag{A6}$$

which is a linear differential equation with respect to $\tau$ having the solution

$$\tau = \exp\left(\int \frac{2dg}{\sqrt{\pi}}\right)\left[C_2 + \int F(g)\exp\left(-\int \frac{2dg}{\sqrt{\pi}}\right)dg\right], \tag{A7}$$

where $F(g)$ is the right-hand side of (A6).

Performing the integration in (A7), we obtain

$$\tau = (1/3\delta_0^2 A)(g^3 + \tfrac{3}{2}\sqrt{\pi}\,g^2 + \tfrac{3}{2}\pi g + \tfrac{3}{4}\pi^{3/2} + C_3) , \tag{A8}$$

which may be considered as a first-order solution $g = g(\tau)$.

(iii) From (A8) we can obtain an explicit determination of $\ddot{g}/\dot{g}^3$, entering the integral expression $J$:

$$A\ddot{g}/\dot{g}^3 = -(1/\delta_0^2)(2g + \sqrt{\pi}) , \tag{A9}$$

and therefore giving a second-order approximation for $J$:

$$\begin{aligned} J^{(2)} &= -\frac{1}{\delta_0^2}\int_0^g (2\tilde{g} + \sqrt{\pi})\exp[-(\tilde{g} - g)^2]d\tilde{g} \\ &= -\frac{1}{\delta_0^2}[1 - \exp(-g^2)] \\ &\quad + \frac{2}{\delta_0^2}(g + \tfrac{1}{2}\sqrt{\pi})\int_0^g \exp(-\tilde{g}^2)d\tilde{g} \\ &\simeq -(1/\delta_0^2)[1 - \exp(-g^2)] + (2/\delta_0^2)(g + \tfrac{1}{2}\sqrt{\pi})\tfrac{1}{2}\sqrt{\pi} . \end{aligned} \tag{A10}$$

In the limit $g \gg 1$ we are led to

$$A/\dot{g} = (1/\delta_0^2)(g^2 + \sqrt{\pi}\,g + \tfrac{1}{2}\pi - 1) , \tag{A11}$$

which integration gives the solution (87).


[1] A. S. Kompaneets, Zh. Eksp. Teor. Fiz. 31, 876 (1956) [Sov. Phys. JETP 4, 730 (1957)].
[2] H. Dreicer, Phys. Fluids 7, 735 (1964).
[3] R. Weymann, Phys. Fluids 8, 12 (1965).
[4] L. M. Kovrizhnykh, Zh. Eksp. Teor. Fiz. 48, 1114 (1965) [Sov. Phys. JETP 21, 744 (1965)].
[5] (a) J. Peyraud, J. Phys. (Paris) 29, 88 (1968); (b) 29, 806 (1968); (c) 29, 872 (1968).
[6] Ya. B. Zel'dovich and E. V. Levich, Zh. Eksp. Teor. Fiz. 55, 2423 (1968) [Sov. Phys. JETP 28, 1287 (1969)].
[7] (a) R. A. Syunyaev and Ya. B. Zel'dovich, Astrophys. Space Sci. 4, 301 (1969); (b) 7, 20 (1970).
[8] Ya. B. Zel'dovich and R. A. Syunyaev, Zh. Eksp. Teor. Fiz. 62, 153 (1972) [Sov. Phys. JETP 35, 81 (1972)].
[9] E. V. Levich, Zh. Eksp. Teor. Fiz. 61, 112 (1971) [Sov. Phys. JETP 34, 59 (1972)].
[10] A. F. Illaronov and R. A. Syunyaev, Astron. Zh. 51, 698 (1974) [Sov. Astron. 18, 413 (1975)].
[11] Ya. B. Zel'dovich and R. A. Syunyaev, Zh. Eksp. Teor. Fiz. 68, 786 (1975) [Sov. Phys. JETP 41, 391 (1976)].
[12] I. K. Krasyuk, P. P. Pashinin, and A. M. Prokhorov, Pis'ma Zh. Eksp. Teor. Fiz. 12, 439 (1970) [JETP Lett. 12, 305 (1970)].
[13] M. Decroisette, J. Peyraud, and G. Piar, Phys. Rev. A 5, 1391 (1972).
[14] Ya. B. Zel'dovich, E. V. Levich, and R. A. Syunyaev, Zh. Eksp. Teor. Fiz. 62, 1392 (1972) [Sov. Phys. JETP 35, 733 (1972)].
[15] A. A. Galeev and R. A. Syunyaev, Zh. Eksp. Teor. Fiz. 63, 1266 (1972) [Sov. Phys. JETP 36, 669 (1973)].
[16] A. V. Vinogradov, Ya B. Zel'dovich, and I. I. Sobel'man, Pis'ma Zh. Eksp. Teor. Fiz. 17, 271 (1973) [JETP Lett. 17, 195 (1973)].
[17] J. R. Albritton, Phys. Fluids 18, 51 (1975).
[18] V. Ya Gol'din, R. A. Syunyaev, and B. N. Chetverushkin, Zh. Eksp. Teor. Fiz. 68, 36 (1975) [Sov. Phys. JETP 41, 18 (1975)].
[19] J. Peyraud and J. Coste, Phys. Rev. A 14, 469 (1976).
[20] C. Montes and J. Peyraud, J. Plasma Phys. 19, 349 (1978).
[21] G. Reinisch, Physica (Utrecht) 81C, 339 (1976).
[22] G. Reinisch, Physica (Utrecht) 83C, 347 (1976).
[23] J. Coste and J. Peyraud, Phys. Rev. A 12, 2144 (1975).
[24] C. Montes, Astrophys. J. 216, 329 (1977).
[25] C. Montes, J. Plasma Phys. 11, 141 (1974).
[26] G. Reinisch and C. Montes, Phys. Rev. A 15, 385 (1977).
[27] For $\nu \gg \nu_p$ [$\nu_p = (n_e e^2/\pi m_e)^{1/2}$ being the plasma frequency] and in the presence of a plasmon turbulence verifying $kT_{\text{turb}}/kT_e > \nu^4/n_e \nu_p c^3$ the linear Raman scattering dominates the Compton and the coefficient $kT_e/h$ in Eq. (5) must be replaced by $(kT_{\text{turb}}/h)(n_e \nu_p c^3/\nu^4)$.
[28] C. Montes, *Plasma Physics: Nonlinear Theory and Experiments* (Plenum, New York, 1977), pp. 222–240.
[29] V. E. Zakharov, S. L. Musher, and A. M. Rubenchik, Zh. Eksp. Teor. Fiz. 69, 155 (1975) [Sov. Phys. JETP 42, 80 (1976)].
[30] S. V. Manakov, Zh. Eksp. Teor. Fiz. 67, 543 (1974) [Sov. Phys. JETP 40, 269 (1975)].
[31] (a) G. Reinisch, Thèse d'Etat (University of Nice, 1976) (unpublished); (b) J. Fernandez and G. Reinisch, Physica 91A, 393 (1978).
[32] (a) C. Montes, J. Peyraud, and M. Hénon, Phys. Fluids 22, 176 (1979); (b) C. Montes, *Lecture Notes in Physics* (Springer-Verlag, Berlin, 1979) Vol. 98, pp. 203–216.
[33] V. G. Makhankov, Phys. Rep. 35 (1), 1–128 (1978).
[34] J. Fernandez and G. Reinisch, Physica (Utrecht) 91A, 393 (1978).